DCO4 LATTICE DESIGN FOR 6.4 KM ILC DAMPING RINGS *

M. Korostelev†, A. Wolski, University of Liverpool and the Cockcroft Institute, UK

Abstract

A new lattice design for the ILC damping ring has been developed since the beginning of 2008 as a lower cost alternative to the previous OCS6 design. The lattices for the electron and positron damping rings are identical, and are designed to provide an intense, 5 GeV beam with low emittance at extraction. The latest design, presented in this paper, provides sufficient dynamic aperture for the large positron beam at injection. The lattice also meets the engineering requirements for arrangement of the positron ring directly above the electron ring in the same tunnel.

INTRODUCTION

The basic requirements for the ILC damping rings have been specified in the Reference Design Report (RDR) [1] as the following: highly stable beam at extraction with horizontal normalized emittance lower than 8 μm and vertical normalized emittance of 20 nm or lower; large acceptance for the injected positron beam coming directly from the positron source (without any pre-damping ring); machine repetition rate of 5 Hz; single tunnel to host both electron and positron rings; low cost for the machine.

A new lattice design for the 6.4 km ILC damping ring (DR), named 'DCO', has been developed since the beginning of 2008 as a lower cost alternative to the previous OCS baseline design, which was based on theoretical minimum emittance arc cells. The DCO design has a 5 GeV racetrack layout with circumference of 6476.4 m (two arcs connected by long straights) where the arcs have a radius of 675 m and consist of identical FODO cells. The DCO lattice was modified several times, with revised versions of the lattice named as DCO2, DCO3 and DCO4. However, the ring circumference and overall racetrack layout of the machine remained the same.

In the DCO2 lattice design, the straight sections were identical, except for the injection section in one straight taking the place of the extraction section in the opposite straight. In March 2009, following a review of the machine configuration, the lattice was modified to provide injection and extraction in the same straight, while the other straight accommodated all the wigglers and RF cavities (DCO3). Finally, in August 2009 further modifications to the dispersion suppressors and injection/extraction sections (driven mainly by engineering requirements) were made, resulting in the DCO4 lattice design.

* Work supported by the Science and Technology Facilities Council.
† maxim.korostelev@stfc.ac.uk

LATTICE PARAMETERS AND LAYOUT

The damping ring consists of two dispersion-free straight sections with wigglers, RF cavities, injection/extraction sections, circumference chicanes, and phase trombones as shown in Fig. 1 (top). Dispersion suppressors link the arcs and the straights.

The key features of the DCO4 layout can be summarized as follows:

- The lattices of the electron and positron damping rings are identical.
- The lattice meets the engineering requirements for arrangement of the positron ring directly above the electron ring in the same tunnel, using common girders for the arc dipoles in the two rings, but with the beams circulating in opposite directions as illustrated in Fig. 1 (bottom).
- The positron injection and electron extraction beam lines are housed together in a single tunnel, as are the electron injection and positron extraction beam lines.
- Because of the large radial size of the RF cryostats, the RF sections are arranged so that the RF cryostats from the different rings do not line up with each other.

Localizing all superconducting elements (wigglers and RF cavities) for the two rings in one straight of the tunnel allows some simplifcation of the systems for providing power and cryogenics.

Variation of the momentum compaction factor α_p from 2.9×10^{-4} to 1.3×10^{-4} can be achieved by tuning the horizontal phase advance per arc cell over a range from 72° to 100°. Table 1 summarizes the main lattice parameters for three different phase advances per arc cell. Notice that the vertical and horizontal phase advances per arc cell are close to each other. The choice of momentum compaction factor is a compromise between various machine parameters, for example, normalized beam emittance $\gamma\epsilon_x$ versus acceptance, or required RF voltage versus instability thresholds (increase of α_p raises the microwave instability threshold) etc.

Each arc consists of 98 identical FODO arc cells with a dispersion suppressor at each end. The FODO arc cell is 21.2 m long and includes one bending magnet with length of 2 m, field 0.262 T and bending angle $2\pi/200$. Using a single dipole per cell simplifies the design and helps to keep the cost of the machine low. One sextupole, skew quadrupole and steering magnet (dipole corrector) are located upstream of each quadrupole in the arc cell. A button

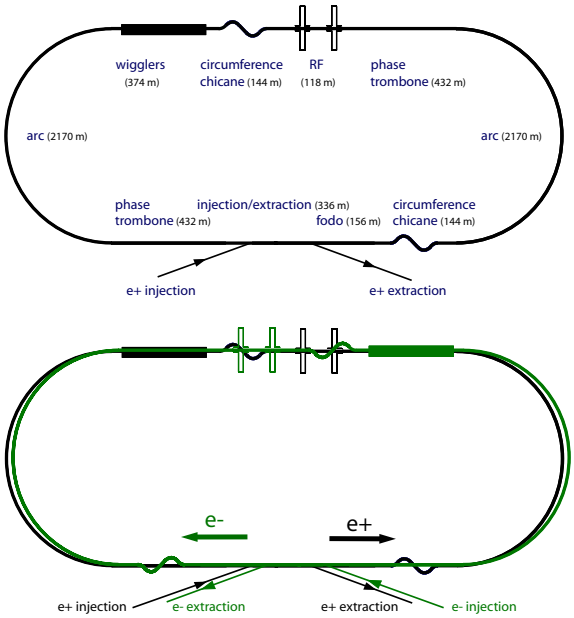

Figure 1: DCO4 layout of the positron damping ring (top). Arrangement of the positron DR (black layout) directly above the electron DR (green layout) in the same tunnel.

Table 1: Main parameters for the DCO4 damping rings lattice.

Circumference	6476.4 m		
Beam energy	5 GeV		
RF frequency	650 MHz		
τ_x/τ_y	21.1 ms		
σ_s	6 mm		
σ_δ	1.27×10^{-3}		
Wiggler	400 mm period; 1.6 T peak field		
Arc cell phase advance	72°	90°	100°
α_p	$2.9 \cdot 10^{-4}$	$1.6 \cdot 10^{-4}$	$1.3 \cdot 10^{-4}$
$\gamma\epsilon_x$	6.4 μm	4.4 μm	3.9 μm
RF voltage	32.6 MV	20.4 MV	17.1 MV
Tunes, ν_x/ν_y	61.12/60.41	71.12/71.41	76.12/75.41
ξ_x/ξ_y	-71.0/-72.6	-89.2/-91.0	-99.8/-100.7

type BPM [2] is located downstream of each quadrupole in the ring. There are 692 quadrupoles in total in the ring. Studies for low-emittance tuning [3] suggest that it should be possible to meet the specifications on the vertical emittance, even if the numbers of BPMs and correctors are reduced.

The phase trombone consists of 36 fodo cells incorporated in 6 periodic groups. Each phase trombone allows a variation of the phase advance across the straight section from $\{-0.5 \div 0.5\} \cdot \pi$ horizontally and $\{-0.2 \div 0.3\} \cdot \pi$ vertically, without any change in the optics in the rest of the straight section.

The circumference chicanes allow adjustment of the circumference of the ring, without any change of the ring RF frequency (which is locked to the main linac). Eight "zigzag" chicanes (four per straight) provide a total circumference adjustability in the range ± 7 mm, with a maximum emittance increase of $\Delta\gamma\epsilon_x = 0.24\,\mu$m.

Fast radiation damping is achieved using a series of 88 superconducting wiggler modules with a length of 2.45 m for each wiggler module. The wigglers for the ILC DR are based on the CESR-c hybrid superconducting wiggler design. They are inserted in a periodic FODO structure (two wiggler modules per FODO) with low vertical beta function to minimize the linear tune shift. A photon absorber [2, 4, 5] is inserted after each wiggler so that the large synchrotron radiation load can be handled safely.

The ring circumference is constrained to 6476.4 m to provide good flexibility for fill patterns for stored bunch trains. At the given circumference and RF frequency, the number of bunches stored in the ring can range from 5265 bunches with population 10^{10} particles and bunch separation 3.1 ns, to 2610 bunches with population 2×10^{10} particles, and separation 6.2 ns. Bunches are extracted and injected individually from/in the ring in the horizontal plane using a fast kicker with rise/fall time ~ 3 ns. The injection septum and injection kicker are separated by a horizontal phase advance of $\pi/2$ (as are the extraction septum and extraction kicker) and inserted in long drifts with low phase advance and high horizontal beta function of ~ 70 m. If the DR is filled with 2610 bunches separated by 4 DR RF buckets in a train, the extraction kicker should pulse with a repetition rate of 2.71 MHz to provide the specified uniform bunch spacing of 369.23 ns in the extraction line, corresponding to 480 linac RF buckets. The injection and extraction are performed simultaneously to reduce variations in beam loading, but the injection kicker starts to pulse on the next turn after the beginning of the extraction. Thus, injected bunches fill the gaps vacated by extracted bunches in the same order as the bunches were extracted. Full refilling of the ring is completed in 46 turns (1 ms).

DYNAMIC APERTURE

The linear and nonlinear optimization for a low emittance lattice is always a compromise between a small final emittance and reasonable dynamic aperture (DA) of the machine. For a racetrack lattice, a particular issue is that sextupoles in the arcs need to be used to correct chromaticity not just in the arcs, but in the straights as well. Local chromaticity can limit the off-momentum DA. In the case of DCO4 with 72° phase advance per arc cell, the arcs contribute about two-third of the natural (linear) chromaticity of the full lattice. Sextupoles for chromatic correction are arranged in two interleaved families in the arcs. The total number of sextupoles (392) is equal to the total number of quadrupoles in the arcs. In the case that the phase advance across each arc cell is close to 90°, the periodicity

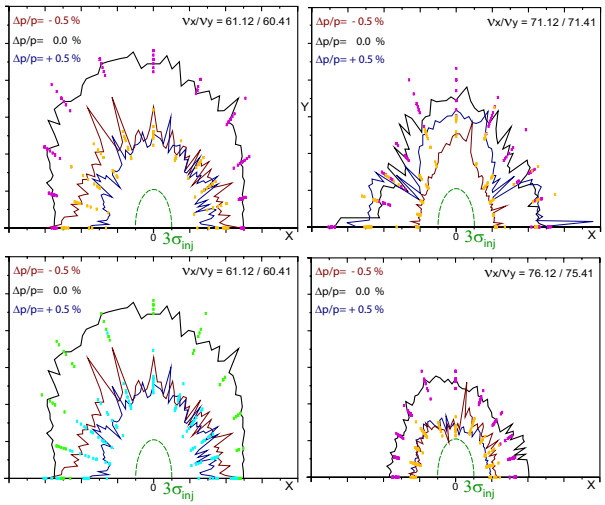

Figure 2: Dynamic aperture of DCO4 lattice with the arc cells tuned to 72° (top-left and bottom-left), 90° (top-right) and 100° (bottom-right).

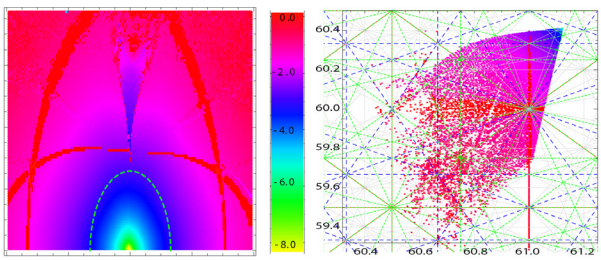

Figure 3: Frequency map for DCO4 lattice tuned to $\nu_x/\nu_y = 61.12/60.41$.

of the lattice leads to an enhancement of the nonlinear effects from the sextupoles, resulting in an unacceptable deterioration of the DA. For this case only, a non-interleaved arrangement of two sextupole families is used, where adjacent sextupoles in each family are separated by a phase advance of 180°. This results in a greatly improved DA. Note that only 152 sextupoles are needed for the non-interleaved arrangement. The horizontal and vertical phase advances between the last FODO cell in one arc and the first FODO cell in the following arc are adjusted to an even multiple of π, to minimize excitation of some phase-dependent terms of high-order geometric aberrations, which can drive octupole resonances.

Fig. 2 shows the on-momentum and off-momentum ($\Delta p/p = \pm 0.5\%$) DA without any lattice errors (solid curves), computed for the three sets of lattice parameters summarized in Table 1. The green dashed ellipses in Figs. 2 and 3 indicate the maximum betatron amplitude for injected positrons with transverse distribution specified by $A_x + A_y < 0.09\,\mathrm{m}\cdot\mathrm{rad}$ where $A_x = 2\gamma J_x$, and J_x is the betatron action. The maximum horizontal and vertical betatron amplitudes in the injected positron beam at the location of the kicker are 25 mm and 7.5 mm, respectively. Assuming a beam with Gaussian distribution at injection, the dashed ellipse represents 3σ of injected beam size. Although the DA decreases with higher phase advance in the arcs, it may still be sufficient at 100° per arc cell, but starts to become unacceptable if the arc cell phase advance is higher than 102°.

Sextupole alignment errors of 80 μm rms generate a normalised vertical emittance of around 20 nm. The magenta points in Fig. 2 show the variations of the footprint of the on-momentum DA computed for ten seeds of random sextupole alignment errors with 80 μm rms. The variations for off-momentum DA at $\Delta p/p = \pm 0.5\%$ computed for the same number of seeds and rms errors are indicated by the yellow points in Fig. 2. Quadrupole alignment errors with 1 μm rms are included in both calculations to generate an rms orbit deviation of 20 μm: this represents the expected accuracy for closed orbit correction. The given alignment errors do not lead to any significant reduction of the DA.

The DA also demonstrates good tolerance to an rms betabeat of $\sim 5\%$, originating from quadrupole relative field errors of 10^{-3} rms. The variations of the on-momentum DA and off-momentum DA computed for six seeds of quadrupole relative field errors of 10^{-3} rms are shown in Fig. 2 (bottom-left) as the light-green and light-blue points, respectively.

A tune scan shows that the DA is optimised if the fractional part of the horizontal and vertical betatron tunes are close to .12 and .41 respectively. A frequency map of the lattice with betatron working point $\nu_x/\nu_y = 61.12/60.41$ and arc cells tuned to 72° is shown in Fig. 3.

CONCLUSION

The DCO4 lattice provides a high degree of flexibility in tuning for different lattice parameters, and achieves a good balance between dynamic aperture for the large positron beam at injection and low beam emittance at extraction. Many options for the fill patterns in stored bunch trains are possible. The lattice meets known engineering specifications, and provides a suitable baseline for the ILC Technical Design Report.

REFERENCES

[1] ILC Reference Design Report (2007), http://www.linearcollider.org/about/Publications/ Reference-Design-Report

[2] M. Korostelev, A. Thorley, A. Wolski et al., "Impedance and single-bunch instabilities in the ILC damping rings," these proceedings (IPAC'10).

[3] K. Panagiotidis, A. Wolski, "Low-emittance tuning simulations for the ILC damping rings," these proceedings (IPAC'10).

[4] O.B. Malyshev, J.M. Lucas, N. Collomb, S. Postlethwaite et al., "Mechanical and vacuum design of wiggler section of ILC DR," these proceedings (IPAC'10).

[5] K. Zolotarev, O.B. Malyshev, M. Korostelev et al., "SR power distribution along wiggler section of ILC DR," these proceedings (IPAC'10).